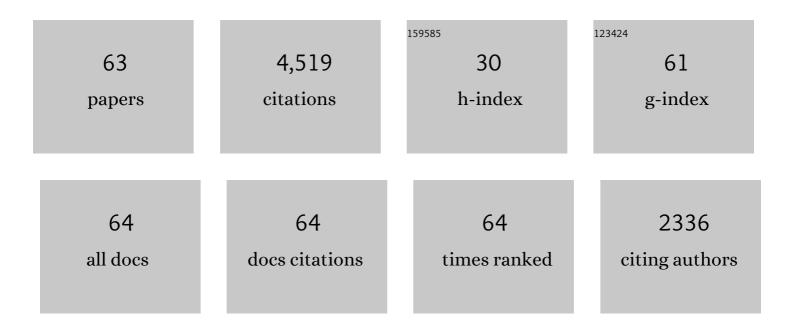
List of Publications by Year in descending order

Source: https://exaly.com/author-pdf/5843525/publications.pdf Version: 2024-02-01



ΥΠΜΑΝ ΖΗΠ

#	Article	IF	CITATIONS
1	Periodic Segregation of Solute Atoms in Fully Coherent Twin Boundaries. Science, 2013, 340, 957-960.	12.6	659
2	The 18R and 14H long-period stacking ordered structures in Mg–Y–Zn alloys. Acta Materialia, 2010, 58, 2936-2947.	7.9	558
3	Texture evolution during static recrystallization of cold-rolled magnesium alloys. Acta Materialia, 2016, 105, 479-494.	7.9	349
4	Precipitation strengthening of aluminum alloys by room-temperature cyclic plasticity. Science, 2019, 363, 972-975.	12.6	323
5	Growth and transformation mechanisms of 18R and 14H in Mg–Y–Zn alloys. Acta Materialia, 2012, 60, 6562-6572.	7.9	233
6	The building block of long-period structures in Mg–RE–Zn alloys. Scripta Materialia, 2009, 60, 980-983.	5.2	182
7	A simulation study of the shape of β′ precipitates in Mg–Y and Mg–Gd alloys. Acta Materialia, 2013, 61, 453-466.	7.9	150
8	Solute clusters and GP zones in binary Mg–RE alloys. Acta Materialia, 2016, 106, 260-271.	7.9	131
9	On the Structure, Transformation and Deformation of Long-Period Stacking Ordered Phases in Mg-Y-Zn Alloys. Metallurgical and Materials Transactions A: Physical Metallurgy and Materials Science, 2014, 45, 3338-3348.	2.2	124
10	Achieving exceptionally high strength in Mg 3Al 1Zn-0.3Mn extrusions via suppressing intergranular deformation. Acta Materialia, 2018, 160, 97-108.	7.9	114
11	Characterization of planar features in Mg–Y–Zn alloys. Acta Materialia, 2010, 58, 464-475.	7.9	99
12	Review of high-strength aluminium alloys for additive manufacturing by laser powder bed fusion. Materials and Design, 2022, 219, 110779.	7.0	94
13	Simulation study of precipitation in an Mg–Y–Nd alloy. Acta Materialia, 2012, 60, 4819-4832.	7.9	84
14	A 12R long-period stacking-ordered structure in a Mg-Ni-Y alloy. Journal of Materials Science and Technology, 2018, 34, 2235-2239.	10.7	83
15	Effects of boron addition on microstructures and mechanical properties of Ti-6Al-4V manufactured by direct laser deposition. Materials and Design, 2019, 184, 108191.	7.0	80
16	Improvement in the age-hardening response of Mg–Y–Zn alloys by Ag additions. Scripta Materialia, 2008, 58, 525-528.	5.2	79
17	<mml:math <br="" altimg="si1.gif" xmlns:mml="http://www.w3.org/1998/Math/MathML">overflow="scroll"><mml:mrow><mml:mrow><mml:mo>{</mml:mo><mml:mrow><mml:mn>10</mml:mn><mml accent="true"><mml:mn>1</mml:mn><mml:mo>Â⁻</mml:mo></mml </mml:mrow><mml:mn>1Twin boundary structures in a Mg–Gd alloy. Acta Materialia, 2018, 143, 1-12.</mml:mn></mml:mrow></mml:mrow></mml:math>	:mrow><ı ın> <td>nml:mover :mrow><mm< td=""></mm<></td>	nml:mover :mrow> <mm< td=""></mm<>
18	Intensive processing optimization for achieving strong and ductile Al-Mn-Mg-Sc-Zr alloy produced by	7.0	72

#	Article	IF	CITATIONS
19	Annealing strengthening in a dilute Mg–Zn–Ca sheet alloy. Scripta Materialia, 2015, 107, 127-130.	5.2	62
20	A closer look at constituent induced localised corrosion in Al-Cu-Mg alloys. Corrosion Science, 2016, 113, 160-171.	6.6	61
21	A simulation study of β 1 precipitation on dislocations in an Mg–rare earth alloy. Acta Materialia, 2014, 77, 133-150.	7.9	60
22	Tilt boundaries and associated solute segregation in a Mg–Gd alloy. Acta Materialia, 2017, 127, 505-518.	7.9	59
23	On the structure and role of <mml:math <br="" xmlns:mml="http://www.w3.org/1998/Math/MathML">altimg="si1.gif" overflow="scroll"><mml:msubsup><mml:mtext>Î²</mml:mtext><mml:mtext>F</mml:mtext><mml:mtext>â€²in Î²1 precipitation in Mg–Nd alloys. Acta Materialia. 2017, 133, 408-426.</mml:mtext></mml:msubsup></mml:math>	nmi:mtex	t> 59 mml:ms
24	Effects of Calcium on Strength and Microstructural Evolution of Extruded Alloys Based on Mg-3Al-1Zn-0.3Mn. Metallurgical and Materials Transactions A: Physical Metallurgy and Materials Science, 2019, 50, 4344-4363.	2.2	54
25	Training high-strength aluminum alloys to withstand fatigue. Nature Communications, 2020, 11, 5198.	12.8	54
26	On the Precipitation in an Ag-Containing Mg-Gd-Zr Alloy. Metallurgical and Materials Transactions A: Physical Metallurgy and Materials Science, 2018, 49, 673-694.	2.2	48
27	Improving Formability of Mg–Ca–Zr Sheet Alloy by Microalloying of Zn. Advanced Engineering Materials, 2016, 18, 1763-1769.	3.5	40
28	Grain boundary α-phase precipitation and coarsening: Comparing laser powder bed fusion with as-cast Ti-6Al-4V. Scripta Materialia, 2022, 207, 114261.	5.2	40
29	Precipitation in a Ag-Containing Mg-Y-Zn Alloy. Metallurgical and Materials Transactions A: Physical Metallurgy and Materials Science, 2016, 47, 927-940.	2.2	38
30	Linear-chain configuration of precipitates in Mg–Nd alloys. Acta Materialia, 2015, 83, 239-247.	7.9	36
31	Effect of solution heat treatment and hot isostatic pressing on the microstructure and mechanical properties of Hastelloy X manufactured by electron beam powder bed fusion. Journal of Materials Science and Technology, 2022, 98, 99-117.	10.7	33
32	Corrosion resistant and high-strength dual-phase Mg-Li-Al-Zn alloy by friction stir processing. Communications Materials, 2022, 3, .	6.9	31
33	A microstructure-based creep model for additively manufactured nickel-based superalloys. Acta Materialia, 2022, 224, 117528.	7.9	29
34	HAADF-STEM study of phase separation and the subsequent α phase precipitation in a β-Ti alloy. Scripta Materialia, 2016, 112, 46-49.	5.2	27
35	Revisiting building block ordering of long-period stacking ordered structures in Mg–Y–Al alloys. Acta Materialia, 2018, 152, 96-106.	7.9	24
36	Origin of non-uniform plasticity in a high-strength Al-Mn-Sc based alloy produced by laser powder bed fusion. Journal of Materials Science and Technology, 2022, 103, 121-133.	10.7	22

#	Article	IF	CITATIONS
37	Microstructure, mechanical behaviour and strengthening mechanisms in Hastelloy X manufactured by electron beam and laser beam powder bed fusion. Journal of Alloys and Compounds, 2021, 862, 158034.	5.5	21
38	In-situ duplex structure formation and high tensile strength of super duplex stainless steel produced by directed laser deposition. Materials Science & Engineering A: Structural Materials: Properties, Microstructure and Processing, 2022, 833, 142557.	5.6	19
39	Dynamic precipitation behavior and mechanical properties of hot-extruded Mg89Y4Zn2Li5 alloys with different extrusion ratio and speed. Materials Science & Engineering A: Structural Materials: Properties, Microstructure and Processing, 2020, 798, 140121.	5.6	17
40	Helium bubble nucleation in Laser Powder Bed Fusion processed 304L stainless steel. Journal of Nuclear Materials, 2020, 542, 152443.	2.7	16
41	Towards creep property improvement of selective laser melted Ni-based superalloy IN738LC. Journal of Materials Science and Technology, 2022, 112, 301-314.	10.7	16
42	Production Strategy for Manufacturing Large-Scale AlSi10Mg Components by Laser Powder Bed Fusion. Jom, 2021, 73, 770-780.	1.9	13
43	Effects of Post Heat Treatments on Microstructures and Mechanical Properties of Selective Laser Melted Ti6Al4V Alloy. Metals, 2021, 11, 1593.	2.3	13
44	Characterisation of intermetallic phases in an Mg–Y–Ag–Zn casting alloy. Philosophical Magazine Letters, 2010, 90, 173-181.	1.2	12
45	Guided Self-Assembly of Nano-Precipitates into Mesocrystals. Scientific Reports, 2015, 5, 16530.	3.3	12
46	On the prismatic precipitate plates in Mg–Ca–In alloys. Scripta Materialia, 2015, 101, 16-19.	5.2	12
47	Atomic-Scale Investigation of the Borides Precipitated in a Transient Liquid Phase-Bonded Ni-Based Superalloy. Metallurgical and Materials Transactions A: Physical Metallurgy and Materials Science, 2020, 51, 1689-1698.	2.2	12
48	(Al,Mg) ₃ La: a new phase in the Mg–Al–La system. Acta Crystallographica Section B: Structural Science, Crystal Engineering and Materials, 2018, 74, 370-375.	1.1	11
49	Incoherent tilt grain boundaries stabilized by stacking faults and solute-cluster segregation: a case-study of an Mg-Gd alloy. Materials Research Letters, 2020, 8, 268-274.	8.7	11
50	Microstructure control by heat treatment for better ductility and toughness of Ti-6Al-4V produced by laser powder bed fusion. Australian Journal of Mechanical Engineering, 2021, 19, 680-691.	2.1	9
51	Characterization and Formation of Rod-Shaped (Al,Si)3Ti Particles in an Al-7Si-0.35Mg-0.12Ti (WtÂPct) Alloy. Metallurgical and Materials Transactions A: Physical Metallurgy and Materials Science, 2015, 46, 3723-3731.	2.2	8
52	A first-principles study of <mml:math <br="" xmlns:mml="http://www.w3.org/1998/Math/MathML">altimg="si1.svg"><mml:msubsup><mml:mrow><mml:mi mathvariant="normal">β</mml:mi </mml:mrow><mml:mtext>F</mml:mtext><mml:mo>′</mml:mo>phase in magnesium-rare earth binary systems. Computational Materials Science, 2019, 170, 109126.</mml:msubsup></mml:math>	msubsup>	
53	Isotropic and improved tensile properties of Ti-6Al-4V achieved by in-situ rolling in direct energy deposition. Additive Manufacturing, 2021, 46, 102151.	3.0	8
54	Atomic-scale study of {1 1 2} twin boundary structure in a β-Ti alloy. Philosophical Magazine Letters, 2016, 96, 280-285.	1.2	7

#	Article	IF	CITATIONS
55	Effect of Deformation Reduction on Microstructure, Texture, and Mechanical Properties of Forged Ti-6Al-4V. Journal of Materials Engineering and Performance, 2021, 30, 1147-1156.	2.5	7
56	On the complex intermetallics in an Al-Mn-Sc based alloy produced by laser powder bed fusion. Journal of Alloys and Compounds, 2022, 901, 163571.	5.5	6
57	Hierarchical layered and refined grain structure of Inconel 718 superalloy produced by rolling-assisted directed energy deposition. Additive Manufacturing Letters, 2021, 1, 100009.	2.1	4
58	The β1 Triad-Related Configurations in a Mg-RE Alloy. Metallurgical and Materials Transactions A: Physical Metallurgy and Materials Science, 2020, 51, 1887-1896.	2.2	3
59	Scanning strategy induced cracking and anisotropic weakening in grain texture of additively manufactured superalloys. Additive Manufacturing, 2022, 52, 102660.	3.0	3
60	Effect of in-situ layer-by-layer rolling on the microstructure, mechanical properties, and corrosion resistance of a directed energy deposited 316L stainless steel. Additive Manufacturing, 2022, 55, 102863.	3.0	3
61	One of the potentially optimal interfaces of β-FeSi2/Si. Journal of Crystal Growth, 2005, 279, 129-139.	1.5	2
62	Making every electron count: materials characterization by quantitative analytical scanning transmission electron microscopy. Microscopy and Microanalysis, 2016, 22, 1430-1431.	0.4	0
63	Influence of Flash Treatment on Pseudoelastic Behaviour of Biomedical Ti-25Nb-3Zr-3Mo-2Sn Alloy. Materials Science Forum, 2016, 879, 1375-1380.	0.3	0